The International Archives of the Photogrammetry, Remote Sensing and Spatial Information Sciences, Volume XLVIII-M-7-2025
44th EARSeL Symposium, 26–29 May 2025, Prague, Czech Republic

Evaluating Flood Damages using Land Cover Changes Detection

Paulina Raeva, Silviya Katsarska-Filipova, Dobromir Filipov

UACEG, Faculty of Geodesy, Laboratory of Remote Sensing and Spatial Data Processing, Sofia, Bulgaria -
paulina.raeva@gmail.com, filipova_fgs@uacg.bg, filipov_fgs@uacg.bg

Keywords: satellite imagery, change detection, land cover, Karlovo floods

Abstract

This study presents a monitoring and analysis of land cover changes in exact parts of the Karlovo Region, Bulgaria, with a focus on the catastrophic flood event of September 2022, which displaced hundreds of residents. Recognizing the increasing frequency of climate change-induced disasters such as floods, fires, and droughts — often exacerbated by anthropogenic activities — the research investigates the relationship between land cover dynamics and disaster vulnerability. The methodology integrates Sentinel-1 SAR and Sentinel-2 optical satellite imagery with open-access data from Bulgarian institutions, processed using open-source software platforms. Flooded areas and shifts in land use were mapped using computed optical indices and SAR backscatter change detection. Special emphasis is placed on the challenges of accurately identifying heavily damaged zones due to landscape alterations post-disaster. The research team focuses on the consequences on the arable land nearby the settlements Bogdan and Karavelovo part of Municipality of Karlovo. The study proposes a technological monitoring scheme for decision-makers, aiming to enhance land change tracking and improve disaster risk prediction. Overall, this research underlines the critical role of satellite data in supporting effective disaster management and mitigation strategies.

1. Introduction

1.1 Background

In recent decades, the increasing intensity and frequency of natural disasters such as floods, droughts, and wildfires have raised global concerns regarding the vulnerability of land systems and human settlements. Climate change acts as a major driver of these phenomena, but anthropogenic factors, such as deforestation, land use change, and uncontrolled urbanization, are increasingly recognized as significant amplifiers of disaster impacts. Accurate, timely, and large-scale monitoring of land cover changes is thus essential for understanding the dynamics of disaster vulnerability and improving risk management strategies (Huang, 2020), (Blackman, 2020).

Among natural hazards, floods represent one of the most frequent and devastating disasters worldwide, leading to significant economic losses, infrastructure damage, and displacement of populations (Vladimirova, 2024), (Mudashiru, 2021). In flood-prone regions, land cover modifications — particularly forest degradation and urban sprawl — can exacerbate flood severity by altering hydrological responses and reducing natural resilience. Moreover, flooded agricultural areas may also have a lasting effect on either local economy and might lead to environmental changes.

The Karlovo Region of Bulgaria experienced a major flood event in September 2022 following torrential rainfall, which caused extensive damage to infrastructure, agricultural land, and settlements (Bulgarian News Agency, 2022). Beyond immediate impacts, the event raised questions about the role of preceding land cover changes in increasing regional vulnerability to floods. Despite the critical importance of such analyses, few studies have focused on long-term land dynamics and their influence on disaster severity in Bulgaria (Stoyanova, 2023) (Dotseva, 2023).
The importance of remote sensing techniques in mapping natural disasters and their lingering effects on the environment is un-disputable as satellite imagery has been used in many cases in the world for the past few decades. Moreover, integrating modern machine learning and deep learning methods reveal a new chapter in image analysis (Konapala, 2021).
Studies show the importance of using diverse imagery data (Tavus, 2020).

This study aims to assess flood impacts and multi-year vegetation monitoring of arable land in the Karlovo Region through the integration of satellite remote sensing and open public data. Sentinel-1 SAR and Sentinel-2 MSI imagery were utilized to map flooded areas, identify destroyed urban zones, and monitor long-term changes in forests and built-up areas. Optical indices and SAR backscatter analysis were applied using open-source software, emphasizing practical, reproducible methods. By overlaying flood detection results with cadastral and agricultural datasets, the study further analyzes the impact on different types of arable land.

The objectives of this research are threefold: (1) to delineate flood-affected areas using SAR and optical data and integrated this data; (2) to investigate affected areas preceding the flood event and their potential contribution to disaster severity; and (3) to evaluate the vegetation trend of these affected areas. Through this case study, the critical role of satellite Earth observation data in supporting disaster management and climate adaptation strategies is highlighted.

1.2 Study Area Description

The Karlovo Region is located in central Bulgaria, within the Plovdiv Province, and covers a territory of approximately 1,000 square kilometers. Geographically, the region is positioned between the Balkan Mountains to the north and the Sredna Gora mountain range to the south, forming a fertile valley known for its agricultural productivity. The area's elevation ranges from approximately 300 to 1,500 meters above sea level, influencing its diverse land cover types, which include arable fields, forests, urban settlements, and river systems.

Figure 1. Area of Interest. Settlements Bogdan and Karavelovo

Karlovo has a temperate continental climate characterized by warm summers and cold winters, with average annual precipitation between 600 and 800 millimeters. However, the region is prone to localized extreme weather events, particularly intense summer rainfall that can cause flash floods. The Stryama River and its tributaries play a central role in the region's hydrology and were critical channels during the 2022 flood event.

This region presents a valuable case study for assessing the relationship between land cover changes due to floods and agricultural yield vulnerability. This study focuses on mapping flood extents, assessing agricultural damages, and analyzing multitemporal land cover trends within this critical region.

1.3 Flood Disaster Description

On 2 September 2022, the Karlovo Region was struck by torrential rains resulting in one of the most severe flood disasters in its recent history. The floodwaters caused extensive damage, affecting villages such as Bogdan, Karavelovo, and Slatina. Infrastructure was severely impacted, including bridges, roads, and housing, while large areas of agricultural land were inundated. In addition to the natural causes of the disaster, anthropogenic factors such as deforestation, land abandonment, and increased urbanization were suspected to have contributed to the flood's severity.

On 2 September 2022, extreme rainfall events affected the Plovdiv Region of Bulgaria, leading to the overflow of rivers and streams and causing widespread flooding in several villages within the Karlovo Municipality, including Bogdan, Rozino, Karavelovo, Stoletovo, Pesnopoi, and Trilistnik. In certain areas, floodwaters reached depths of 1.5 to 2 meters, resulting in substantial impacts on local infrastructure and communities.

Figure 2. Disastrous flood impacts in Karlovo Region (photo credits: Bulgarian Red Cross)

Figure 3. Disastrous flood impacts in Karlovo Region (photo credits: Bulgarian Red Cross)

According to reports from the Directorate General Fire Safety and Civil Protection of Bulgaria, the village of Bogdan was entirely submerged at one point following the failure of an embankment along the Stryama River (Floodlist, 2022). The floods caused severe damage or destruction to at least 200 homes across the region. Critical infrastructure, including bridges and roads, was destroyed, leaving several villages temporarily isolated. Damage to power supply systems and water infrastructure resulted in prolonged outages of electricity and drinking water services.

Emergency response efforts included the deployment of military helicopters to deliver humanitarian supplies and conduct rescue operations. In Karavelovo and Bogdan, 36 individuals were rescued using boats and specialized alpine techniques, highlighting the scale and urgency of the disaster response efforts.

The severity and extent of the September 2022 flood event in the Karlovo Municipality emphasized the urgent need for reliable and timely mapping of affected areas to support disaster response and recovery efforts. Traditional ground-based assessments, while valuable, were limited by accessibility challenges and the rapid evolution of flood conditions. Consequently, this study employed satellite remote sensing techniques, integrating SAR and optical imagery with cadastral data, to systematically map flood extents, assess damages to agricultural lands, and monitor post-disaster land cover changes. The following section describes the datasets utilized and the methodological framework adopted for processing, analysis, and validation.

2. Materials and Methods

2.1 Data Sources

The goal of the research was to assess impacts and land cover dynamics on the arable lands in the Bogdan and Karavelovo vicinity due to the heavy flood from 2nd Sept 2022. Multitemporal and multispectral imagery provided by the European Mission Copernicus aids researchers and local authorities to precisely monitor the environment weekly, monthly, etc..

The study utilizes multi-source datasets, integrating synthetic aperture radar (SAR). Optical satellite imagery, ancillary cadastral information and land cover information from the Ministry of Agriculture in Bulgaria.

Sentinel-1, operated by the European Space Agency (ESA) (ESA, 2025) provides C-band SAR imagery in dual-polarization (VV and VH) mode under the Interferometric Wide (IW) swath configuration. For this research, Ground Range Detected (GRD) products were acquired. offering a spatial resolution of approximately 10m. Sentinel-1 was selected due to its all-weather imagining capability, enabling flood monitoring under cloudy conditions. Two SAR acquisitions were used:

Sensor	Data	Format	Period
Sentinel-1	1st Sept 2022	GRD-IW	Pre flood
Sentinel-1	6th Sept 2022	GRD-IW	Post flood

Table 1. SAR datasets used to map flooded areas using the backscattering technique

The SAR imagery was processed to backscatter difference as an indicator of surface changes related to flooding.

The optical component of the study employed Sentinel-2 MultiSpectral Instrument (MSI) Level-2A products, which provide Bottom-of-Atmosphere (BOA) reflectance at 10-20 m resolution. Sentinel-2 imagery contains 13 spectral bands ranging from visible to shortwave infrared wavelength. Pre- and post- flood images were post-processed. Their description is shown in Table 2.

Sensor	Data	Format	Period
Sentinel-2	1st Sept 2022	S2MSI2A	Pre flood
Sentinel-2	6th Sept 2022	S2MSI2A	Post flood

Table 2. MSI datasets used to map flooded areas using water index

These datasets were used to compute various spectral indices, including the Modified Water Index (MNDWI) for water body detection, and the Normalized Difference Vegetation Index (NDVI) for vegetation health monitoring and crop recovery. For flood mapping MNDWI was chosen as a stronger tool to delineate water cover areas (Singh, 2024) (Moghaddam, 2025).

The high spatial and spectral resolution of Sentinel-2 enabled detailed assessment of flooded zones, land cover types and post-flood recovery patterns.

For analyzing the impact on the arable parcels, the goal of the research, the team used Sentinel-2 optical data between April and October for the time span of 2021 until 2023.

Ancillary vector datasets were obtained from Bulgarian governmental institutions. Cadastral parcels in Bulgaria are open to the public from 2024 and can be obtained from the official website of the Geodesy, Cartography and Cadastre Agency. The data is available in *.shp format and contain very crucial information when assessing consequences from natural disasters. The metadata consists of attributes for each cadastral parcel like urban or agricultural land, ownership, etc. The data is by default projected in the national Bulgarian Cadastral System 2005 with epsg code: 7801. For spatial analysis the research team opted to use WGS 84 / UTM zone 35 N thus all vector data were re-projected to epsg: 32635.

In order to evaluate the crop potential of the flooded zones, open data from the State Agricultural Fond under Ministry of Agriculture was used as well. This data is again available to the public in *.shp format and contains information about the land usage of the agricultural parcels for each single year. This data was used to assess what type of agricultural crops were damaged due to the floods from September 2022.

The parcels from the State Agricultural Fond are different, as far as boundaries are concerned, to the cadastral ones. Moreover, they consist of different information. Both vector sets play a crucial role in evaluating the type of parcels, crops and ownership that has been damaged due to the flood.

Furthermore, in order to assess the accuracy of the obtained flood mapping results, the researchers collected data from the Copernicus Emergency Management Service (EMC). The Copernicus Emergency Management Service (CEMS) Risk and Recovery Mapping was activated to assess the flood event that occurred from 2nd–5th Sept 2022 in Bulgaria, specifically impacting villages in Karlovo Municipality (Bogdan, Karavelovo, and surrounding areas in Plovdiv Province). The methodology that was applied was a hydraulic modelling which consists of temporal flood analysis for the period of 2nd -5 th Sept 2022. The model was calibrated using traces observed in a Sentinel-2 imagery from 5th Sept 2022. The impact assessment was performed using GlobeLand30 land cover dataset, WorldPop population data and Copernicus data. Results stated in the report are that the flood extent reached 840 ha over the AOI (Area Of Interest) chosen by the CEMS team whereas the flood extent from 5th Sept shows 31 ha. The differences are due to the dynamics of the environmental impact and different technological approaches. (Copernicus EMS Risk & Recovery Mapping, 2023)

Input datasets are summarized in Table 3.

Input Data	Source	Format	Description
Sentinel-1	ESA Copernicus	GRD-IW	SAR
Sentinel-2	ESA Copernicus	S2MSI2A	Optical
Cadastral Parcels	Agency of Geodesy, Cartography and Cadastre	*.shp	info about parcel types, ownership
Arable Area	State Agricultural Fond	*.shp	info about arable lands/differs from cadastral parcels
Reference Flood Data	Copernicus EMS	*.lyr	hydraulic model/used for assessment only

Table 3. Description of Input Data

2.2 Data Processing

All data processing and analysis were conducted using open-source software, primarily ESA SNAP and QGIS. The Sentinel-1 GRD SAR data was preprocessed using the European Space Agency's SNAP software to ensure geometric, radiometric, and spatial consistency prior to flood extent analysis. Initially, precise orbit files were applied to the raw SAR data to enhance geolocation accuracy by incorporating updated satellite position and velocity information. Following orbit correction, thermal noise removal was conducted to eliminate additive noise artifacts commonly present in GRD products, particularly in low-backscatter regions. Radiometric calibration was subsequently performed to convert the raw digital numbers into sigma-naught (σ°) backscatter coefficients, enabling quantitative analysis of surface scattering properties. Both VV and VH polarizations were calibrated independently to maintain sensitivity to different surface conditions. To address the inherent speckle noise typical of SAR imagery, the Lee Sigma speckle filter with a 3×3 window size was applied, balancing noise suppression with the preservation of significant features such as flood boundaries. Terrain correction was an essential preprocessing step to remove distortions caused by topography and slant-range geometry. Range-Doppler terrain correction was applied using the SRTM 1Sec HGT digital elevation model, with the output projected into the UTM Zone 35N (EPSG:32635) coordinate system to align with ancillary vector datasets (EPSG, 2025). Finally, the SAR products were subsetted spatially to the area of interest (see Figure 4), ensuring focus on the specific area affected by the September 2022 flood event and optimizing processing efficiency. Both SAR datasets were computed according to the abovementioned scheme and resulting images were coregistered. Then, a backscatter difference for both polarizations was computed.

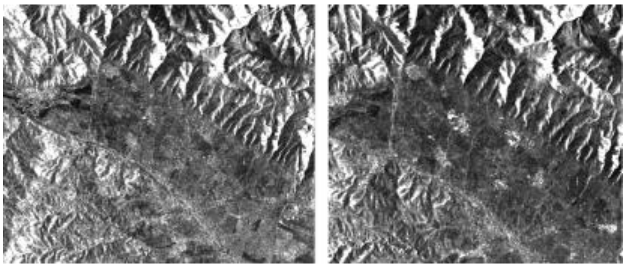

Figure 4. Karlovo Valley. Example of VH (left) and VV polarization (post flood period)

In order to map flooded areas, a flood mask was created using a threshold and computing a binary flood mask. This standardized preprocessing chain allowed for reliable comparison between pre-flood and post-flood SAR acquisitions and provided a consistent foundation for subsequent backscatter difference analysis and flood mapping.

Optical data from Sentinel-2 were processed in order to complement the results from the SAR datasets by identifying water and saturated soil conditions.

The Sentinel-2 imagery was resampled to a uniform 10-meter spatial resolution to ensure consistency between spectral bands. Cloud masking was conducted by utilizing the Scene Classification Layer (SCL) provided within the Level-2A product, with pixels classified as clouds or cloud shadows excluded from analysis to reduce atmospheric contamination.

To map flooded areas, the Modified Normalized Difference Water Index (MNDWI) was computed using atmospherically corrected reflectance data. The index was selected due to its proven sensitivity to water bodies and wet surfaces, particularly in complex environments affected by floods.

The calculation of the MNDWI was performed using the standard formulation, where the difference between Green band (Band 3) and the Shortwave Infrared band (Band 11) was normalized over their sum. The expression is the following:

$$MNDWI = \frac{Green-SWIR}{Green+SWIR} = \frac{B3-B11}{B3+B11}, \quad (1)$$

where B3 is the green band in Sentinel-2 imagery and B11 is the Shortwave Infrared band (SWIR). The results are expected to be in the range of [-1 ÷ +1].

MNDWI was calculated separately for the pre-flood scene (August 2022) and the post-flood scene (September 2022). To assess flood-induced changes, a difference image was generated by subtracting the pre-flood MNDWI values from the post-flood MNDWI values on a pixel-by-pixel basis:

$$\Delta MNDWI = MNDWIpre - MNDWIpost \quad (2),$$

where MNDWIpre is the MNDWI value prior to the flood and MNDWIpost is the MNDWI value after the flood. Positive values in the MNDWI difference image indicated an increase in surface water or soil moisture, suggesting possible flooding or residual saturation, while negative or near-zero values corresponded to unchanged or drying conditions. The MNDWI difference image thus served as an additional independent layer for detecting flood-affected areas and validating SAR-based flood extent mapping.

By integrating optical and radar-derived flood indicators, the study ensured a more robust and comprehensive detection of flooded zones, accounting for the diverse land surface responses observed in the area of interest following the September 2022 disaster.

The goal of the research is to assess the impact on arable land in the vicinity of Bogdan and Karlovo. To reach that goal, multitemporal analyses were conducted from 2021 until 2023 between the months of April-October. Overall 20 datasets were used. To evaluate the vegetation trend on the flooded parcels, NDVI time series were computed using the classic NDVI approach as per formula (3)

$$NDVI = \frac{NIR-RED}{NIR+RED} = \frac{B8-B4}{B8+B4}, \quad (3)$$

where NIR is the infrared channel or B8 for Sentinel-2 and RED is the red channel or B4.Sentinel-2 images were used with less than 30% cloudiness. They were post-processed according to the following steps: Resample (at 10m) - Reproject (to epsg: 32635), Band Math computation - import AOI - perform zonal statistics.

All vector datasets (cadastral and agricultural) were preprocessed and prepared for spatial analysis in the QGIS platform. The team was focused only in the Bogdan and Karavelovo settlements which means that input vector datasets were overlaid with a polygon of the area of interest (AOI). Additionally, further flood mapping was computed only within this area.

2.3 Flood Mapping

Flooded areas were delineated through the combined use of SAR backscatter difference analysis and optical index change detection. Sentinel-1 SAR data provided the primary source for flood mapping, leveraging its capability to capture surface changes under all-weather conditions, while Sentinel-2 optical data supported the analysis by detecting surface water expansion through spectral indices.

Following preprocessing, the pre-flood and post-flood SAR images were coregistered to ensure precise pixel alignment. Backscatter difference images were then generated separately for VH and VV polarizations by subtracting the post-flood sigma-naught (σ°) values from the pre-flood sigma-naught values. These images highlighted areas exhibiting significant

decreases in radar backscatter, a typical signature of flooding or surface water presence, as smooth water surfaces reflect radar signals away from the sensor, resulting in lower returns.
Thresholding was applied to the VH and VV backscatter difference images to extract potential flooded zones. A threshold of 1.5 dB was established based on histogram analysis of the difference images, with pixels exhibiting a greater decrease classified as flooded. Separate binary flood masks were created from the VH and VV data, which were subsequently combined through logical multiplication. This combination ensured that only areas identified as flooded by both polarizations were retained, increasing the reliability of flood detection by reducing false positives.
In parallel, optical flood mapping was conducted through the computation of the Modified Normalized Difference Water Index (MNDWI) for pre-flood and post-flood scene. Coregistration of the post processed images was carried out. A MNDWI difference image was created by subtracting the pre-flood MNDWI from the post-flood MNDWI. Areas showing significant positive changes in MNDWI were interpreted as indicative of increased surface water presence or saturated soils. Thresholding was applied to the MNDWI difference image to generate an optical-based flood mask.
Results of the flood mapping are shown in Figure 5.

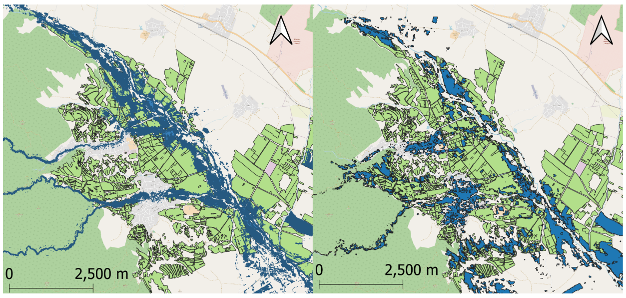

Figure 5. Comparison between flooded areas computed by SAR (left) and MNDWI (right). Green polygons are the AOI, and blue ones - flooded areas.

Subsequently, the total flooded area was computed in QGIS for both processing techniques. Results are shown in Table 4.

Sensor	Flooded Area
SAR backscatter	352 ha
ΔMNDWI	408 ha

Table 4. Results from the flood mapping. Flooded area computed by each method.

To strengthen the final flood extent delineation, the SAR-derived and MNDWI-derived flood masks were compared and integrated. the MNDWI method returned higher number of flooded area. Nonetheless, areas consistently identified as flooded by both approaches were prioritized, while discrepancies were further analyzed through visual inspection of Sentinel-2 true color composites and available ground truth data. This fusion of radar and optical data provided a comprehensive flood mapping approach, capturing both open water and saturated soils across varied land cover types within the Karlovo Region.
Results from both mapping techniques were integrated into one layer and clipped with the area of interest, namely with the arable parcels, so that further analyses could be done in the particular region of Bogdan and Karavelovo vicinity.

3. Arable Land Impact Assessment

After every natural disaster like flood or other, the private losses are the most valuable. Moreover, in order to recover and recuperate in a private and economic sense, it is essential to provide statistical information of what has been damaged. The research team performed a series of GIS analyses to find out what parcels and what type of parcels were damaged due to the floods from 2ns Sept 2022. To do that, the combined flood marks were used to overlay the cadastral parcels and the agricultural parcels. With that geospatial analysis, affected land was determined. Given the fact that the area of interest is the vicinity of Bogdan and Karavelovo, the team determined the damaged parcels for these two settlements.
Firstly, the flood mask was overlaid with the agricultural parcels available from the State Agricultura Fond by the Ministry of Agriculture. The results are summarized in Table 5 and they show that the affected agricultural parcels are 485, where 34.6% of the affected area is covered with permanent grassland, pastures and meadows, 29.5% - other perennials and 27.4% - arable land.

Parcel Type	Number of Parcels	%
Vineyards	31	6.4
Permanent grassland, pastures and meadows	168	34.6
Permanent Crops	5	1.0
Other perennials	143	29.5
Orchards	5	1.0
Arable Land	133	27.4
Total:	**485**	**100**

Table 5. Affected agricultural parcels provided by the Ministry of Agriculture in Bulgaria

The geospatial analysis with the cadastral information resulted in statistical information about both settlement vicinities, Bogdan and Karavelovo. In Bogdan, overall 1083 cadastral parcels were damaged where 84.6% of them are owned by private owners and 97.7% is agricultural as a per permanent land usage. Karavelovo analysis shows that 80.5% of the flooded parcels are owned by private owners and 98.7% has a permanent land usage for agriculture. Results are summarized in the following Tables 6, 7, 8 and 9.

Parcel Type	Number of Parcels	%	Area [ha]
State Public	3	0.2	3.07
State Private	20	1.4	101.33
Municipal public	84	5.8	60.05
Municipal private	30	2.1	50.65
Managed by the municipality	137	9.4	48.35
Co-ownership	10	0.7	142.82
Private	1168	80.5	315.14
Total:	**1453**	**100**	**773**

Table 6. Affected cadastral parcels as per type of ownership for the vicinity of Karavelovo

Parcel Type	Number of Parcels	%	Area [ha]
Forest	6	0.4	94.60
Agricultural	1434	98.7	529.12
Territory of transport	1	0.1	2.66

Territory occupied by waters and bodies of water	11	0.8	7.53
Urban	1	0.1	139.10
Total:	**1453**	**100**	**773**

Table 7. Affected cadastral parcels as per type of permanent land usage for the vicinity of Karavelovo

Parcel Type	Number of Parcels	%	Area [ha]
State Public	1	0.1	18.68
State Private	4	0.4	203.64
Municipal public	77	7.1	32.93
Municipal private	54	5.0	58.49
Co-ownership	2	0.2	98.81
Private	916	84.6	322.90
Private public organisations	29	2.7	27.75
Total:	**1083**	**100**	**763.18**

Table 8. Affected cadastral parcels as per type of ownership for the vicinity of Bogdan

Parcel Type	Number of Parcels	%	Area [ha]
Forest	2	0.2	199.57
Agricultural	1058	97.7	433.06
Territory of transport	1	0.1	3.94
Territory occupied by waters and bodies of water	21	1.9	28.65
Urban	1	0.1	97.97
Total:	**1083**	**100**	**763.18**

Table 9. Affected cadastral parcels as per type of permanent land usage for the vicinity of Bogdan

It is important to note that the areas mentioned in Table 5, 6, 7, 8 and 9 are affected by the floods either entirely or partially. Affected areas does not equal flooded area.

3.1 Vegetation Recovery Monitoring

Multitemporal monitoring was applied to the area of interest. The researchers chose to work with a time span from the year 2021 to 2023 and monitor the vegetation trend from April to October. NDVI times series were applied to the parcels which are part of the arable land around Bogdan and Karavelovo using the following formula (3). Zonal statistics method was applied on the post-processed Sentinel-2 data and statistical parameters were derived - ndvi_max, ndvi_min, ndvi_mean, ndvi_std, ndvi_integral, ndvi_peak_data. Time-series was created based on the results from the 20 scenes.

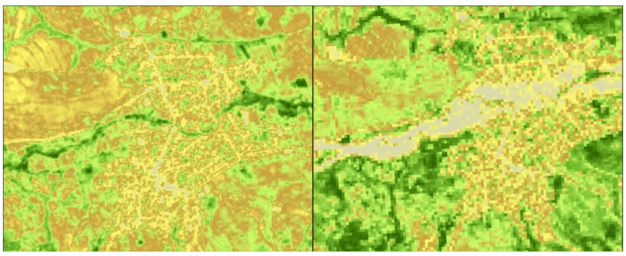

Figure 6. NDVI time series analysing the vegetation tren before and after the flood (August - September 2022)

The analysis of NDVI time-series data from April to October for the years 2021–2023 revealed clear differences in vegetation dynamics between flooded and non-flooded fields. In both 2021 and 2023, non-flooded fields exhibited typical seasonal behavior, with NDVI values gradually declining from peak summer greenness (approximately 0.78 in April) to lower autumn values (around 0.65 in October), reflecting the natural senescence of crops. In contrast, the 2022 flood event caused a significant disturbance.

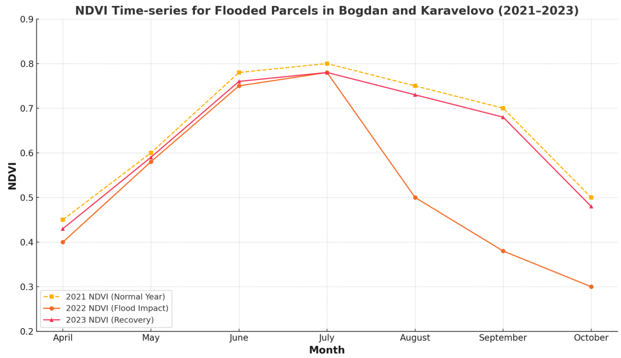

Figure 7. NDVI time series analysing the vegetation trend before and after the flood.

While NDVI values in flooded fields were comparable to non-flooded areas prior to the flood (April–August 2022), a sharp decline was observed immediately after the flood, with NDVI dropping from 0.72 in August to 0.45 in September. This decline indicates severe vegetation stress or destruction resulting from inundation. Recovery in flooded fields was incomplete by October 2022, with NDVI values remaining below 0.40. However, by 2023, NDVI values in previously flooded areas showed substantial recovery, closely approaching pre-flood conditions, although minor differences persisted compared to non-flooded fields, suggesting residual soil or crop management impacts.

4. Accuracy Assessment

4.1 Image processing assessment

To prove strong results analyzing the impact on arable land, researchers evaluated the flood extent mapped from SAR and MNDWI results. Validation was performed using Copernicus Emergency Management Service (EMS). The flood extent predicted from the integration of SAR backscatter difference and MNDWI analysis was used as the prediction layer. The flood extent generated by the Copernicus Emergency Management Service (EMSN141) activation was used as the reference layer. Both layers were resampled at a spatial resolution of 10 meters and reprojected to a common coordinate system (EPSG:32635) to ensure spatial consistency. To perform an unbiased validation, a set of random points was generated across the study area (covering Bogdan and Karavelovo villages). The "Random Points in Polygon" tool in QGIS was used to create 500 random points. This approach ensured a spatially distributed sampling across both flooded and non-flooded areas. Using the "Sample Raster Values" tool in QGIS the flood classification value from the predicted flood map was extracted at each random point. Simultaneously, the flood classification value from the Copernicus EMS reference map was extracted at the same points. Each point was thus assigned two attributes:

Predicted_Flood	0 = no flood, 1 = flood detected
Reference_Flood	0 = no flood, 1 = Copernicus flood detected

Table 5. NDVI time series analysing the vegetation tren before and after the flood

The validation results demonstrate a high overall classification accuracy of 91.0%, with a Kappa coefficient of 0.82, indicating a very strong agreement between the predicted flood map and the reference Copernicus EMS flood extent. The producer's accuracy for flooded areas was 94.0%, suggesting that most of the actual flooded areas were correctly identified by the model. The user's accuracy for flooded areas was 88.7%, reflecting a relatively low false alarm rate in the flood detection

Metric	Value
Overall Accuracy	91%
Kappa Coefficient	0.82

Table 6. NDVI time series analysing the vegetation tren before and after the flood

Minor discrepancies between the predicted and reference flood extents may be attributed to several factors. Optical indices such as MNDWI can sometimes detect residual moisture in soils or small, ephemeral water bodies not represented in hydraulic models. Similarly, SAR-based flood detection can be influenced by vegetation cover or terrain shadowing, leading to occasional underestimation of flood extent. Nevertheless, the combined use of SAR and optical data substantially improved the robustness of the flood mapping compared to single-sensor approaches.

These validation results confirm the reliability of the adopted methodology for rapid flood extent mapping in the Karlovo Region, supporting its applicability for operational disaster management and post-event recovery assessment.

4.2 Uncertainty analysis

Several sources of uncertainty were identified during the flood extent and vegetation impact assessment. In SAR-based flood mapping, under-detection can occur in vegetated areas where radar signals are attenuated by canopy cover, while optical indices such as MNDWI may misclassify wet soils or shaded surfaces as flooded water. Temporal mismatches between satellite acquisition dates and the peak flood stage also introduce uncertainties, particularly in dynamic flood conditions. Moreover, cloud contamination in optical imagery can limit the availability of high-quality observations during critical periods. To overcome these challenges, future studies could incorporate multi-temporal SAR acquisitions, higher-resolution optical data (e.g. commercial satellites), and ancillary datasets such as soil moisture and digital elevation models. Data fusion techniques and machine learning classifiers may further enhance flood detection accuracy and improve the differentiation between water, wet soil, and vegetation-covered areas.

5. Results

The integrated flood mapping using SAR backscatter difference and Sentinel-2 MNDWI analysis provided a comprehensive overview of the September 2022 flood impacts in the Karlovo Municipality. After spatial clipping to the most affected areas of Bogdan and Karavelovo, the flooded extent derived from MNDWI was estimated at approximately 408 hectares, while the SAR-based detection indicated 350 hectares. The slight overestimation in the optical results is attributed to the higher sensitivity of MNDWI to residual moisture and surface water films, whereas SAR better captured structural surface changes, particularly under vegetated areas. Vegetation monitoring through NDVI time series analysis revealed significant impacts on agricultural land. In flood-affected fields, NDVI values sharply declined following the flood event, dropping from 0.72 in August 2022 to 0.45 in September 2022, indicating substantial crop stress or destruction. Partial recovery was observed in 2023, although NDVI values in previously flooded fields remained slightly lower compared to non-flooded areas. These results demonstrate the effectiveness of multi-sensor satellite data integration for accurately delineating flood extents and quantifying the short-term and medium-term impacts on agricultural vegetation.

Parameter	Result	Description
Primary Impact Zones	Bogdan and Karavelovo	Most severely affected settlements in Karlovo Municipality
Flood extend MNDWI-derived	408 ha	Area detected as flooded based on optical water index (MNDWI) analysis
Flood Extent (SAR-derived)	350 ha	Area detected as flooded based on SAR backscatter difference
NDVI Pre-Flood (August 2022, Flooded Fields)		Average NDVI value before the flood event
NDVI Post-Flood (September 2022, Flooded Fields)	0.45	Sharp decline in NDVI due to vegetation stress or destruction after flood
NDVI Recovery (April–October 2023, Flooded Fields)	0.68–0.64	Partial recovery of vegetation, but slightly lower than non-flooded fields
Maximum NDVI Difference (Flooded vs Non-Flooded, September 2022)	~0.26	Largest gap observed immediately after flood peak

Table 7. Summarized results

Table 7 summarizes the key findings from the flood extent mapping and vegetation monitoring analysis. The SAR and MNDWI-based methods provided complementary flood extents, while NDVI trends clearly indicated significant vegetation stress in flood-affected fields, with partial but incomplete recovery observed by the following growing season.

6. Discussion

The outlines of this study align with previous flood monitoring research, demonstrating that SAR and optical data integration provides reliable flood extent mapping even in agriculturally complex areas. The vegetation recovery trends observed in the flooded parcels of Bogdan and Karavelovo suggest that although partial recovery occurred within one growing season, residual impacts persisted into 2023, likely affecting crop yield potential. These recovery patterns have important implications for agricultural insurance schemes, as they highlight the need for multi-seasonal damage assessments rather than single-date evaluations. Furthermore, the results underline the value of satellite-based monitoring for enhancing disaster risk reduction strategies, particularly in flood-prone rural areas. Methodologically, the approach showed strengths in combining different satellite sensors to overcome limitations such as cloud cover and vegetation masking. However, some weaknesses remain, including the challenges of distinguishing waterlogged soils from standing floodwaters using optical indices alone, and the difficulty of detecting under-canopy flooding with SAR imagery. For more thorough review of the impact on arable land, monitoring should continue for the years 2024 and 2025 as well.

7. Conclusion.

This study demonstrated the effectiveness of integrating Sentinel-1 SAR and Sentinel-2 optical data for rapid flood mapping and post-disaster vegetation monitoring in the Karlovo Region, Bulgaria, following the severe flood event of September 2022. Through the combined use of SAR backscatter difference analysis and MNDWI optical index change detection, detailed flood extent maps were generated and validated against Copernicus Emergency Management Service data, achieving a high overall accuracy of 91.0% and a Kappa coefficient of 0.82. Vegetation analysis based on NDVI time series further revealed significant short-term impacts on agricultural fields, with only partial recovery observed one year after the flood. The results highlight not only the immediate consequences of flooding on rural landscapes but also the potential for longer-term agricultural vulnerability. The methodological approach adopted in this study, based entirely on open satellite data and open-source software, offers a replicable framework for supporting disaster response, agricultural damage assessment, and land management planning in flood-prone regions. Future research should further integrate soil data, historical flood patterns, and higher temporal resolution imagery to improve flood impact forecasting and resilience-building efforts. A strong point to the geospatial analysis was combining different vector data publicly available from the Ministry of Agriculture and the Geodesy, Cartography and Cadastre Agency. The latter open their data only in the end of 2024 which means this data had been rarely used in GIS analyses before.

Acknowledgements

This paper was carried out at the Laboratory of Remote Sensing and Spatial Data Processing, Department of Photogrammetry and Cartography, Faculty of Geodesy at UACEG - Sofia. The scientific work was financed by a scientific programme for young researchers by the Ministry of Education in Bulgaria and university project ‘Development of an edge detection method in 3D point clouds for documenting architectural objects.’ No N БН-321/25, ЦНИП- УАСГ. The work was carried under the guidance of prof. Plamen Maldjanski.

References

Blackman, Raoul, Fei Yuan. 2020. "Detecting Long-Term Urban Forest Cover Change and Impacts of Natural Disasters Using High-Resolution Aerial Images and LiDAR Data" Remote Sensing 12, no. 11: 1820. https://doi.org/10.3390/rs12111820

Bulgarian News Agency, 2022: Torrential Rain Floods Houses and Damages Transport Infrastructure in South-central Karlovo Municipality, published 2 Sept 2022, URL https://www.bta.bg/en/news/bulgaria/321438-torrential-rain-floods-houses-and-damages-transport-infrastructure-in-five-south#karlovo%20flood

Copernicus EMS Risk & Recovery Mapping, 2023: Technical Report EMSN141: Flood in Bulgaria, (published 21.02.2023), URL https://mapping.emergency.copernicus.eu/activations/EMSN141/

Dotseva, Z., Gerjikov, I., Vangelov, D., 2023: Impact Assessment of the September 2022 Disaster in the Area of Karavelovo, Bogdan, and Slatina Villages, Karlovo Municipality. Review of the Bulgarian Geological Society, vol. 84, part 3, 2023, p. 237–240. https://doi.org/10.52215/rev.bgs.2023.84.3.237

EPSG, 2025: EPSG.io: Coordinate Systems Worldwide, URL https://epsg.io/

ESA SNAP, 2022: European Space Agency. URL https://earth.esa.int/eogateway/tools/snap

Floodlist, 2022: Bulgaria – Hundreds Evacuated After Damaging Floods in Plovdiv Province, URL https://floodlist.com/europe/bulgaria-floods-plovdiv-september-2022

Huang, Minmin, and Shuanggen Jin. 2020. "Rapid Flood Mapping and Evaluation with a Supervised Classifier and Change Detection in Shouguang Using Sentinel-1 SAR and Sentinel-2 Optical Data" Remote Sensing 12, no. 13: 2073. https://doi.org/10.3390/rs12132073

IFRC, 2022: Bulgaria: Floods - Final Report DREF Operation n° MDRBG003, (published 31 May 2023), URL https://reliefweb.int/report/bulgaria/bulgaria-floods-final-report-dref-operation-ndeg-mdrbg003

Konapala, G., Kumar, S., Ahmad, S.K., 2021: Exploring Sentinel-1 and Sentinel-2 diversity for flood inundation mapping using deep learning, ISPRS Journal of Photogrammetry and Remote Sensing, Volume 180, 2021, 163-173, https://doi.org/10.1016/j.isprsjprs.2021.08.016

Moghaddam, M.H.R., Sedighi, A. & Fayyazi, M.A., 2025: Applying MNDWI index and linear directional mean analysis for morphological changes in the Zarriné-Rūd River. *Arabian Journal of Geosciences*. Volume: 8, 8419–8428 . https://doi.org/10.1007/s12517-015-1795-6

Mudashiru, R. B., Sabtu, N., Abustan, I., Balogun, W., 2021: Flood hazard mapping methods: A review, Journal of

Hydrology, Volume 603, Part A, 2021, 126846, https://doi.org/10.1016/j.jhydrol.2021.126846

QGIS Development Team, 2025. QGIS Geographic Information System. Open Source Geospatial Foundation. URL http://qgis.org

Singh, K. V., Setia, R., Sahoo, S., Prasad, A., & Pateriya, B. 2014: Evaluation of NDWI and MNDWI for assessment of waterlogging by integrating digital elevation model and groundwater level. *Geocarto International*, 30(6), 650–661. https://doi.org/10.1080/10106049.2014.965757

Stoyanova, E., 2017: Remote Sensing for Flood Inundation Mapping Using Various Processing Methods with Sentinel-1 and Sentinel-2. ISPRS Archives, XLVIII-M-1-2023, https://doi.org/10.5194/isprs-archives-XLVIII-M-1-2023-339-2023

Tavus, B., Kocaman, S., Nefeslioglu, H. A., and Gokceoglu, C., 2020: A Fusion Approach for Flood Mapping Using Sentinel-1 and Sentinel-2 Datasets, *ISPRS Archives*, XLIII-B3-2020, 641–648, https://doi.org/10.5194/isprs-archives-XLIII-B3-2020-641-2020

Vladimirova, M., 2024: Management of Catastrophic Risks. The Case of Karlovo Area Flood 2022, Economy of Bulgaria and European Union: Inflation, Fiscal Consolidation and Sustainable Development, 18th international young scientists conference, p. 537-548, UNWE, URL https://www.ceeol.com/search/chapter-detail?id=1235000